Article

Comparison of the ATP Binding Sites of Protein Kinases Using Conformationally Diverse Bisindolylmaleimides

Stephen Bartlett, Godfrey S. Beddard, Richard M. Jackson, Veysel Kayser, Colin Kilner, Andrew Leach, Adam Nelson, Peter R. Oledzki, Peter Parker, Gavin D. Reid, and Stuart L. Warriner

J. Am. Chem. Soc., **2005**, 127 (33), 11699-11708• DOI: 10.1021/ja050576u • Publication Date (Web): 02 August 2005

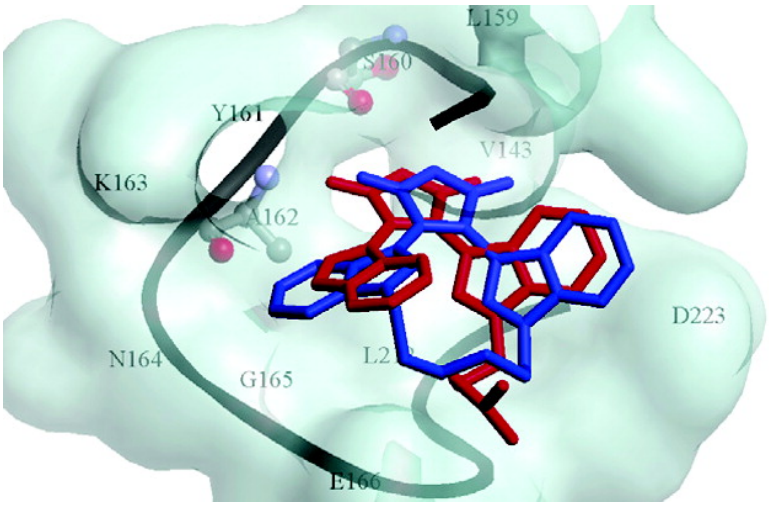

More About This Article

Additional resources and features associated with this article are available within the HTML version:

- Supporting Information
- Links to the 3 articles that cite this article, as of the time of this article download
- Access to high resolution figures
- Links to articles and content related to this article
- Copyright permission to reproduce figures and/or text from this article

View the Full Text HTML

Journal of the American Chemical Society is published by the American Chemical Society. 1155 Sixteenth Street N.W., Washington, DC 20036

J|A|C|S
ARTICLES
Published on Web 08/02/2005

Comparison of the ATP Binding Sites of Protein Kinases Using Conformationally Diverse Bisindolylmaleimides

Stephen Bartlett,[†,‡] Godfrey S. Beddard,[†,‡,§] Richard M. Jackson,[‡,||] Veysel Kayser,[†,§] Colin Kilner,[†] Andrew Leach,[⊥] Adam Nelson,*[,†,‡] Peter R. Oledzki,[‡,||] Peter Parker,[#] Gavin D. Reid,[†,§] and Stuart L. Warriner[†,‡]

Contribution from the School of Chemistry, University of Leeds, Leeds, LS2 9JT, UK, Astbury Centre for Structural Molecular Biology, University of Leeds, Leeds, LS2 9JT, UK, Centre for Chemical Dynamics, University of Leeds, Leeds, LS2 9JT, UK, School of Biochemistry and Microbiology, University of Leeds, Leeds, LS2 9JT, UK, AstraZeneca, Mereside, Alderley Park, Macclesfield, Cheshire, SK10 4TG, UK, and Protein Phosphorylation Laboratory, London Research Institute, 44 Lincoln's Inn Fields, London WC2 3PX, UK

Received January 28, 2005; E-mail: a.s.nelson@leeds.ac.uk

Abstract: The conformation of a bisindolylmaleimide may be controlled by the size of a macrocyclic ring in which it is constrained. A range of techniques were used to demonstrate that the tether controls both the ratio of the two limiting conformers (syn and anti) in solution and the extent of conjugation between the maleimide and indole rings. Screening the conformationally diverse bisindolylmaleimides against a panel of protein kinases allowed their ATP binding sites to be compared using a chemical approach which, like sequence alignment, does not require detailed structural information. This approach lead to the conclusion that several AGC group protein kinases (including PKCα, PKCβ, MSK1, p70 S6K, PDK-1, and MAPKAP-K1α) may be best inhibited by bisindolylmaleimides which adopt a compressed approximately C_2-symmetric anti conformation; in constrast, GSK3β may be best inhibited by bisindolylmaleimides whose ground state is a distorted syn conformation. It is concluded that PDK-1, whose structure has been determined by X-ray crystallography, and its mutants, may serve as particularly useful surrogates for the study of PKC inhibitors.

1. Introduction

The phosphorylation of proteins, which serves as a ubiquitous means for controlling cellular processes, is catalyzed by the protein kinases which account for about 2% of human genes.[1] Protein kinases mediate signal transduction in eukaryotes and can regulate metabolism, transcription, cell cycle progression, and cytoskeletal rearrangement.[1] In addition, protein phosphorylation plays a critical role in cell movement and apoptosis, in intercellular communication during development and in the functioning of the nervous and immune systems. Inhibiting the action of individual protein kinases selectively has therapeutic value, and the first kinase inhibitors, Gleevec and Iressa, have entered the market.[2]

Conformationally diverse molecules are valuable tools in the discovery and optimization of chemical and biological function.[3] Structural features such as ring size, configuration, and substitution can, under either kinetic or thermodynamic control, determine the configuration of new stereogenic centers and axes.[4,5] In addition, these features can also perturb conformation, for example, by controlling the inter-ring torsion angle of biaryl rings, which may have a significant effect on function.[4−7] For example, the catalytic activity and enantioselectivity of bisphosphine (Tunaphos[6]) and binaphthyl (NOBIN[7]) ligands may be tuned through substitution and by constraining the biaryl axis within a medium or large ring. The antibiotic, vancomycin,[5b] and the anticancer and antiviral compound pterocaryanin C[5c] have embedded biaryl axes whose configuration and conformation have a critical effect on their biological activity. Similarly, the configuration and conformation of atropoisomeric amides may be controlled by constraining the axis within a medium ring, and these effects may be used to rationalize the potency of tachykinin NK_1 receptor antagonists.[5d−e]

[†] School of Chemistry, University of Leeds.
[‡] Astbury Centre for Structural Molecular Biology, University of Leeds.
[§] Centre for Chemical Dynamics, University of Leeds.
[||] School of Biochemistry and Microbiology, University of Leeds.
[⊥] AstraZeneca.
[#] London Research Institute.

(1) Manning, G.; Whyte, D. B.; Martinez, R.; Hunter, T.; Sudarsanam, S. *Science* **2002**, *298*, 1912.
(2) Metz, W. M. *Bioorg. Med. Chem. Lett.* **2003**, *13*, 2953.
(3) For example, see: Schreiber, S. L. *Bioorg. Med. Chem.* **1998**, *6*, 1127.
(4) (a) Spring, D. R.; Krishnan, S.; Blackwell, H. E.; Schreiber, S. L. *J. Am. Chem. Soc.* **2002**, *124*, 1354. (b) Carbonnelle, A.-C.; Zhu, J. *Org. Lett.* **2002**, *2*, 3477. (c) Cristau, P.; Vors, J.-P.; Zhu, J. *Tetrahedron* **2003**, *59*, 7859; (d) Krishnan, S.; Schreiber, S. L. *Org. Lett.* **2004**, *6*, 4021.
(5) For example, see: (a) Clayden, J. *Chem. Commun.* **2004**, 127. (b) Nicolaou, K. C.; Boddy, C. N. C.; Brase, S.; Winssinger, M. *Angew. Chem., Int. Ed. Engl.* **1999**, *38*, 2097. (c) Quideau, S.; Feldman, K. S. *Chem. Rev.* **1996**, *96*, 6, 475. (d) Albert, J. S.; Ohnmacht, C.; Bernstein, P. R.; Rumsey, W. L.; Aharony, D.; Masek, B. B.; Dembofsky, B. T.; Koether, G. M.; Potts, W.; Evenden, J. L. *Tetrahedron* **2004**, *60*, 4337. (e) Ishichi, Y.; Ikeura, Y.; Natsugari, H. *Tetrahedron* **2004**, *60*, 4481. (f) Clayden, J.; Lund, A.; Vallverdu, L.; Helliwell, M. *Nature* **2004**, *431*, 966.
(6) (a) Zhang, Z.; Qian, H.; Longmire, J.; Zhang, X. *J. Org. Chem.* **2000**, *65*, 6223. (b) Lei, A.; Wu, S.; He, M.; Zhang, X. *J. Am. Chem. Soc.* **2004**, *126*, 1626.
(7) (a) Lipshutz, B. H.; Shin, Y.-J. *Tetrahedron Lett.* **2000**, *41*, 9515. (b) Lipschutz, B. H.; Buzard, D. J.; Olsson, C.; Noson, K. *Tetrahedron* **2004**, *60*, 4443.

The indolocarbazole alkaloids, such as staurosporine (**1**), K252a (**2**), and rebeccamycin (**3**), are potent, broad spectrum inhibitors of many protein kinases.[8] The indolocarbazole alkaloids function by competing for the ATP binding site of protein kinases and typically have sub-10 nM inhibitory activity. X-ray crystal structures of several kinase−staurosporine complexes have been determined including those of glycogen synthase kinase-3β (GSK3β),[9] cAMP-dependent kinase (cAPK),[10,11] the cyclin dependent kinase CDK2,[10,12] the lymphocyte-specific kinase Lck,[13] the checkpoint kinase Chk1,[14] and the carboxy-terminal Src kinase Csk.[15] The structures reveal that, in each case, staurosporine is bound in the ATP-binding pocket of the kinase and that its lactam mimics the adenine ring of ATP. Despite their broad range of action, the indolocarbazoles have been useful leads in the discovery of selective kinase inhibitors. For example, 7-hydroxystaurosporine (or UCN-01) is more selective than staurosporine for Chk1 and has undergone clinical trials as a kinase inhibitor for the treatment of patients with refractory neoplasms.[16]

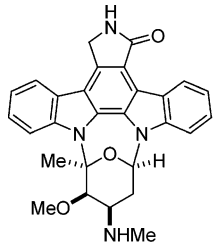

1

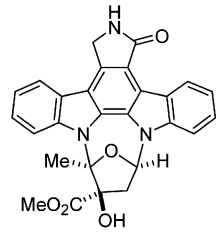

2

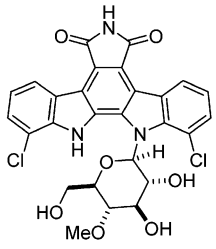

3

A fruitful strategy has been to disrupt the planarity of the indolocarbazole ring system to give either bisindolylmaleimides[17] (e.g., **4**) or dianilinophthalimides[18] (e.g., **5**). The selectivity and potency of some inhibitors of therapeutically important kinases have been refined by the formation of macrocyclic analogues of **4**; for example, the bisindolylmaleimide LY333531 selectively inhibits[19] the β isoforms of protein kinase C (PKCβ) (IC_{50} = 4.7 nM for PKCβI and 5.9 nM for PKCβII), and the macrocyclic analogues **7** target glycogen synthase kinase-3β (GSK3β) (with IC_{50} = 22 nM).[20] PKCβ is

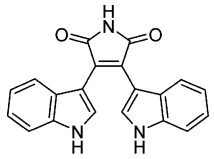

4

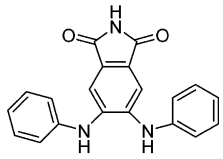

5

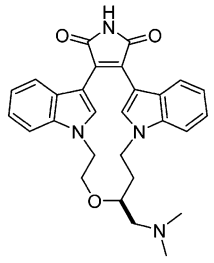

6

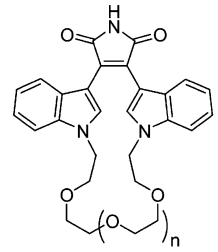

7

selectively activated by elevated glucose in many vascular tissues, and the bisindolylmaleimide **6** can produce significant improvements in diabetic retinopathy, nephropathy, neuropathy, and cardiac dysfunction.[21,22] Indeed, the bisindolylmaleimide **6** is in phase III clinical trials as a therapeutic agent for preventing diabetes complications[23] (such as diabetic retinopathy) and left ventricular hypertrophy in heart failure.[24] GSK3β is involved in the induction of mammalian neurogenesis, and selective ligands for GSK3β may allow the mechanisms that control stem cell fate to be elucidated.[25] The role of GSK3 inhibition in insulin action also makes this a potential therapeutic target in diabetes. Very recently, the mechanism of action of bisindolylmaleimides has been revealed in molecular detail: structures of the complexes of **10** with PKA[26] (Protein Kinase A) and **6**, **8**, **9a**, **9b**, and **10** with PDK-1[27] (3-phosphoinositide-dependent protein kinase-1) have been determined.

The lack of specificity of the indolocarbazole alkaloids generally renders them poor tools for studying protein kinases. Here, we describe a family of macrocyclic bisindolylmaleimides whose diversity stems from the quite distinct regions of conformational space which they populate.[28] The compounds

(8) For reviews, see: (a) Rueegg, U. T.; Burgess, G. M. *Trends Pharm. Sci.* **1989**, *10*, 218. (b) Omura, S.; Sasaki, Y.; Iwai, Y.; Takeshima, H. *J. Antibiot.* **1995**, *48*, 535.
(9) Bertrand, J. A.; Thieffine, S.; Vulpetti, A.; Cristiani, C.; Valsasina, B.; Knapp, S.; Kalisz, H. M.; Flocco, M. *J. Mol. Biol.* **2003**, *333*, 393.
(10) Toledo, L. M.; Lydon, N. B. *Structure* **1997**, *5*, 1551.
(11) Prade, L.; Engh, R. A.; Girod, A.; Kinzel, V.; Hube, R.; Bossemeyer, D. *Structure* **1997**, *5*, 1627.
(12) Lawrie, M. A.; Noble, E. M.; Tunnah, P.; Brown, N. R.; Johnson, L. N.; Endicott, J. A. *Nat. Struct. Biol.* **1997**, *4*, 796.
(13) Zhu, Z.; Kim, J. L.; Newcomb, J. R.; Rose, P. E.; Stover, D. R.; Toledo, L. M.; Zhao, H.; Morgenstern, K. A. *Structure* **1999**, *7*, 651.
(14) Zhao, B.; Bower, M. J.; McDevitt, P. J.; Zhao, H.; Davis, S. T.; Johanson, K. O.; Green, S. M.; Concha, N. O.; Zhou, B.-B. S. *J. Biol. Chem.* **2002**, *277*, 46609.
(15) Ogawa, A.; Takayama, Y.; Sakai, H.; Chong, K. T.; Takeuchi, S.; Nakagawa, A.; Nada, S.; Okada, M.; Tsukihara, T. *J. Biol. Chem.* **2002**, *277*, 14351.
(16) Jackson, J. R.; Gilmartin, A.; Imburgia, C.; Winkler, J. D.; Marshall, L. A.; Roshak, A. *Cancer Res.* **2000**, *60*, 566.
(17) (a) Bit, R. A.; Davis, P. D.; Elliott, L. H.; Harris, W.; Hill, C. H.; Keech, E.; Kumar, G.; Maw, A.; Nixon, J. S.; Vessey, D. R.; Wadsworth, J.; Wilkinson, S. E. *J. Med. Chem.* **1993**, *36*, 21. (b) Toullec, D.; Pianetti, P.; Coste, H.; Bellevergue, P.; Grand-Perret, T.; Ajakane, M.; Baudet, V.; Boissin, P.; Boursier, E.; Loriolle, F.; Duhamel, L.; Charon, D.; Kirilovsky, J. *J. Biol. Chem.* **1991**, *266*, 15771.
(18) Buchdunger, E.; Trinks, U.; Mett, H.; Regenass, U.; Müller, M.; Meyer, T.; McGlynn, E.; Pinna, L. A.; Traxler, P.; Lydon, N. B. *Proc. Natl. Acad. Sci. U.S.A.* **1994**, *91*, 2334.
(19) (a) Jirousek, M. R.; Gillig, J. R.; Gonzalez, C. M.; Heath, W. F.; McDonald, J. H., III; Neel, D. A.; Rito, C. J.; Singh, U.; Stramm, L. E.; Melikian-Badalian, A.; Baevsky, M.; Ballas, L. M.; Hall, S. E.; Winneroski, L. L.; Faul, M. M. *J. Med. Chem.* **1996**, *39*, 2664. (b) Heath, W. F., Jr.; Jirousek, M. R.; McDonald, J. H., III; Rito, C. J. *Eur. Pat. Appl.* **1995**, 657458.
(20) Kuo, G.-H. et al. *J. Med. Chem.* **2003**, *46*, 4021.
(21) Way, K. J.; Katai, N.; King, G. L. *Diabetic Medicine* **2001**, *18*, 945.
(22) Goekjian, P. G.; Jirousek, M. R. *Curr. Med. Chem.* **1999**, *6*, 877.
(23) Nakamura, J. et al. *Diabetes* **1999**, *48*, 2090.
(24) Vlahos, C. J.; McDowell, S. A.; Clerk, A. *Nat. Rev. Drug Discov.* **2003**, *2*, 99.
(25) Ding, S.; Wu, T. Y. H.; Brinker, A.; Peters, E. C.; Hur, W.; Gray, N. S.; Schultz, P. G. *Proc. Natl. Acad. Sci. U.S.A.* **2003**, *100*, 7632.
(26) Gassel, M.; Breitenlechner, C. B.; König, N.; Huber, R.; Engh, R. A.; Bossemeyer, D. *J. Biol. Chem.* **2004**, *279*, 23679.
(27) Komander, D.; Kular, G. S.; Schüttelkopf, A. W.; Deak, M.; Prakash, K. R. C.; Bain, J.; Elliott, M.; Garrido-Franco, M.; Kozikowski, A. P.; Alessi, D. R.; van Aalten, D. M. F. *Structure* **2004**, *12*, 215.
(28) Bartlett, S.; Nelson, A. *Org. Biomol. Chem.* **2004**, *2*, 2874.

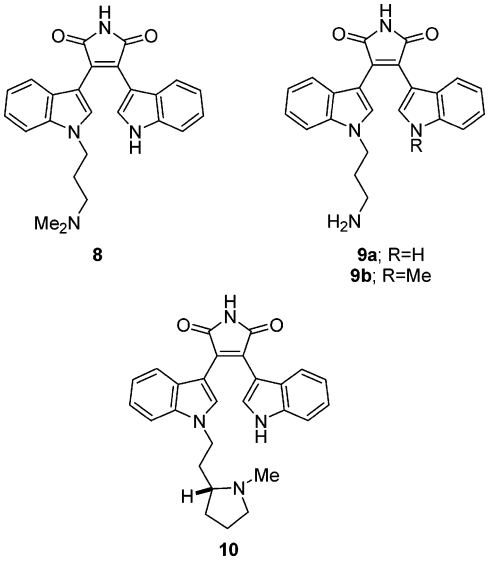

may be used to compare the diversity and similarity of protein kinases in a chemical fashion. Furthermore, the approach may allow the conformations of ligands which are best recognized by particular protein kinases to be identified.

2. Results

We have prepared a family of bisindolylmaleimides **11-*n***, **13** and **15**. The bisindolylmaleimides **11** are macrocyclic analogues in which the length of the tether, $n = 6$ to 10, was varied.[19,28] The bisindolylmaleimides **11-*n*** and **13** were deprotected to give **12-*n*** and **14**.[28]

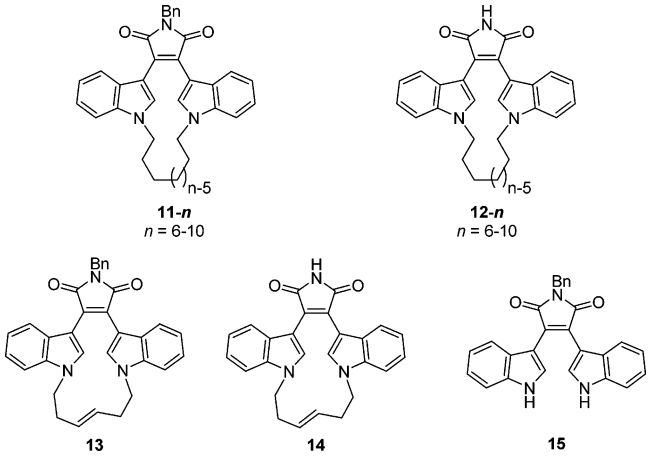

The most striking feature of the macrocycles **11-*n*** was the variation in their color as a function of the length of the tether. In dichloromethane, $\lambda_{max}^{abs} = 505$ nm for **11**−**6** but is between 478 and 488 nm for **11**−**7** to **11**−**10**; two examples are shown in Figure 1, and the data for all of the macrocycles **11** are listed in Table S1, Supporting Information. Formally, the chromophore consists of the two indole rings conjugated with the bridging double bond of the maleimide ring; however, twisting of the rings relative to one another will change conjugation and, hence, the absorption spectra. The conformation of indole rings relative to the maleimide may depend on the tether's length, and any change in conjugation would change the absorption spectrum.

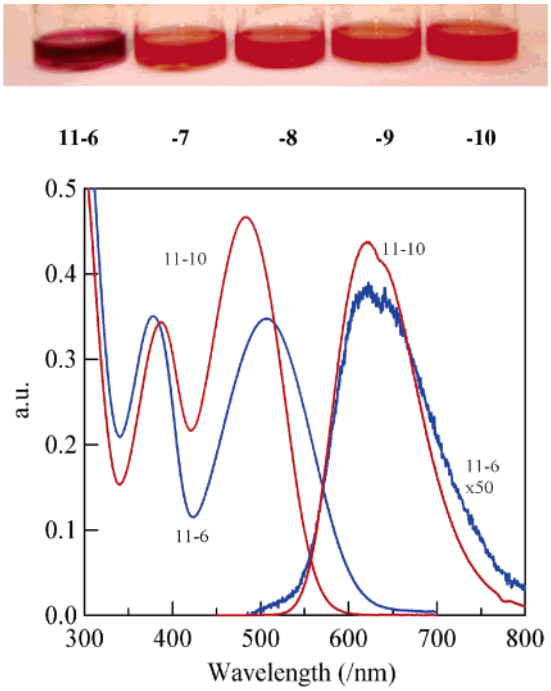

Figure 1. Solutions of the macrocyclic bisindolylmaleimides **11-*n*** (n = 6−10) in chloroform (12.5 mM) and absorption and emission spectra of **11-6** (blue lines) and **11-10** (red lines).

Table 1. Inhibition of Protein Kinase C β(PKC β) by the Bisindolylmaleimides **12-*n***

compound	K_i[a]/nM
12-6	45 ± 10
12-7	790 ± 100
12-8	280 ± 50
12-9	160 ± 30
12-10	580 ± 50

[a] The data fitted a competitive inhibition model with $K_m = 40$ μM for ATP.

The longest wavelength absorption spectra have a shape typical of charge transfer (CT),[29] i.e., an inverted Gaussian shape without significant vibronic features. Additionally, the polar CT nature of the excited state is indicated by the sensitivity of λ_{max}, but not the shape of the spectrum, to solvent dielectric constant: for **11**−**6**, for example, the absorption and emission maxima are, respectively, 462 and 572 nm in hexane ($\epsilon = 1.9$) and 477 and 624 nm in dichloromethane ($\epsilon = 9.1$) which represents an increase in stabilization of ~770 cm^{-1} in the more polar solvent, doubling to 1440 cm^{-1} in acetonitrile ($\epsilon = 37$).

The probable conformational differences between the bisindolylmaleimides **12** led us to investigate their relative ability to inhibit protein kinases. The bisindolylmaleimides **12-*n*** were potent PKCβ inhibitors which were competitive[30] for the ATP binding site. In view of the known mechanism[8,10−15] of inhibition of kinases by staurosporine, this is hardly surprising. However, the potency varied as a function of tether length: PKCβ was inhibited by **12-6** with $K_i = 45$ nM and **12-8** with $K_i = 280$ nM, whereas **12-7** (with $K_i = 790$ nM) was about 20-fold less active than **12-6**; see Table 1 for other values.

The specificity of the bisindolylmaleimides **11-*n***, **12-*n***, **14**, and **15** was determined by screening against a panel of twenty

(29) Turro, N. J. *Modern Molecular Photochemistry*; University Science Books; Sausalito, CA, 1991.
(30) Cleland, W. W. *Methods Enzymol.* **1979**, *63*, 103.

Table 2. Inhibition of Selected Protein Kinases by the Macrocyclic Bisindolylmaleimides **12-*n*** and **14**

	% inhibition with 10 μM inhibitor[a] (estimated K_i/μM)[b]					
kinase	**12-6**	**12-7**	**12-8**	**12-9**	**12-10**	**14**
MSK1	87 (1)	72 (3)	74 (2)	66 (3)	71 (3)	91 (0.6)
PKCα	94 (0.3)	60 (3)	53 (4)	60 (3)	38 (8)	98 (0.1)
p70 S6K	86 (0.9)	72 (2)	58 (4)	59 (4)	69 (2)	90 (0.6)
PDK1	73 (2)	37 (9)	37 (9)	24 (15)	34 (10)	67 (2)
MAPKAP-K1α	89 (1)	58 (5)	45 (9)	56 (5)	45 (9)	88 (1)
GSK3β	90 (0.7)	82 (1.4)	98 (0.2)	98 (0.2)	86 (1.0)	85 (1)

[a] The average of two runs is reported. Typical error: ±5%. [b] Estimated from the relation $V = V_{max}[ATP]/([ATP] + K_m(1 + [I]/K_i))$ on the assumption of competitive inhibition.

nine other protein kinases (see Table S2, Supporting Information).[31] Low levels of inhibition were observed with most of these kinases, suggesting that only the flat indolocarbazole ring system of staurosporine could be accommodated in their ATP binding site. However, significant levels of inhibition of GSK3β (glycogen synthase kinase 3β), MSK1 (nuclear mitogen- and stress-activated kinase-1), p70 S6K (40S ribosomal protein S6 kinase), PDK1, MAPKAP-K1α (MAP kinase-activated protein kinase), PKCα (Protein kinase C α), and SGK (serum- and glucocorticoid protein kinase) were observed with some of the compounds, Table 2 and Table S2, Supporting Information.

The potency of inhibition varied significantly as a function of the tether length. For example, the most potent inhibitors of some of the AGC (cAMP-dependent protein kinase/protein kinase G/protein kinase C) protein kinase extended family were the macrocyclic bisindolylmaleimides **12-6** and **14** with six-atom tethers: of the compounds used in this study, **12-6** and **14** were the most potent inhibitors of MSK1, PDK1, PKCα , PKC β, p70 SGK, and MAPKAP-K1α. The pattern of inhibition of GSK3β was entirely different, with the bisindolylmaleimides **12-8** and **12-9** being the most potent inhibitors. The known binding mode[8,10−15] of staurosporine to protein kinases involves its secondary amide acting as a hydrogen bond donor, and it was surprising to observe, therefore, that some of the *N*-benzyl imides **11** were potent and reasonably selective inhibitors of SGK, Table S2 (Supporting Information).

The physical and biological properties of the bisindolylmaleimides **12** depended on the length of their tethers. In particular, the absorption maxima, λ_{max}^{abs}, and the ability to inhibit particular protein kinases varied throughout the series of compounds. In certain cases, different properties of the compounds appeared to be correlated: for example, the bisindolylmaleimides **12-6** and **14** had the longest wavelength absorption maxima, λ_{max}^{abs}, and were also the most potent inhibitors of the protein kinases, PKCα, PKCβ, and MSK1. In view of the apparent correlation between absorption maxima and the ability to inhibit particular protein kinases, the conformations of the bisindolylmaleimides were investigated in more detail.

Scheme 1. Limiting Conformations of Tethered Bisindolylmaleimides

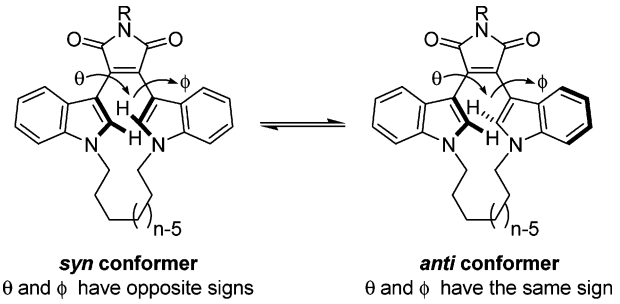

Effect of the Tether on the Conformation and Populations of the syn and anti Conformers. X-ray crystallography and molecular modeling were used to determine the effect of tethers on the conformation of the syn and anti conformers. The detailed conformations of bisindolylmaleimides may be described in terms of the dihedral angles θ and ϕ, Figure 2 (describing the dihedral angles between the indole C_2—C_3 bonds and the maleimide C═C bond). There are two limiting conformations of the bisindolylmaleimides which may be populated: a syn conformer, for which θ and ϕ have opposite signs, and an anti conformer, for which θ and ϕ have the same sign, Scheme 1. Conformations which were observed by X-ray crystallography (left panel, Figure 3; and Table S3) or were revealed by molecular modeling to be significantly populated (right panel, Figure 3, and Table S4) are shown in the Ramachandran-type plots in Figure 3.

Both X-ray crystallography and molecular modeling indicate that, provided that the tether is sufficiently long, the conformation of the syn conformer is unsymmetrical and is similar to that of the unsubstituted compound **15** (for which the dihedrals $\theta = 33°$ and $\phi = -153°$ were observed by X-ray crystallography, and $\theta = 31°$ and $\phi = -153°$ were predicted by molecular modeling). With $n = 8$, the observation of three distinct distorted syn conformers by X-ray crystallography may suggest that a rather shallow potential energy landscape is accessible. With $n = 7$, more severe distortion of the syn conformer of **12-7** was observed: both X-ray crystallography ($\theta = 48°$ and $\phi = -46°$) and molecular modeling ($\theta = 46°$ and $\phi = -46°$) revealed a syn conformer which was approximately C_s-symmetrical.

The effect of the tether on the conformation of the anti conformer was more subtle. Approximately C_2-symmetric anti conformers of **12-7** and **12-8** were identified by molecular modeling: the inter-ring torsion angles, θ and ϕ, were between

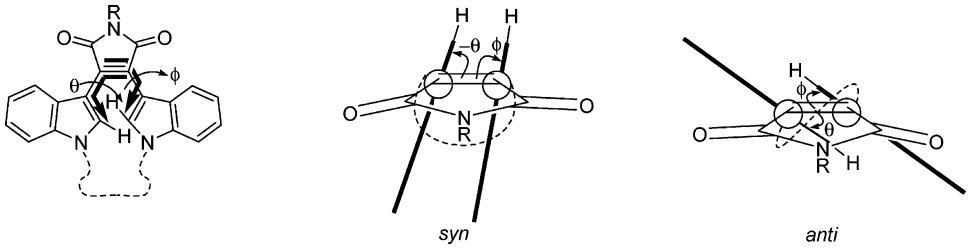

Figure 2. Definitions of the dihedral angles θ and ϕ, and diagrams of top views of the syn and the anti conformers; the tether is shown as a dotted line, and side-on views of the indole rings are shown as thick lines.

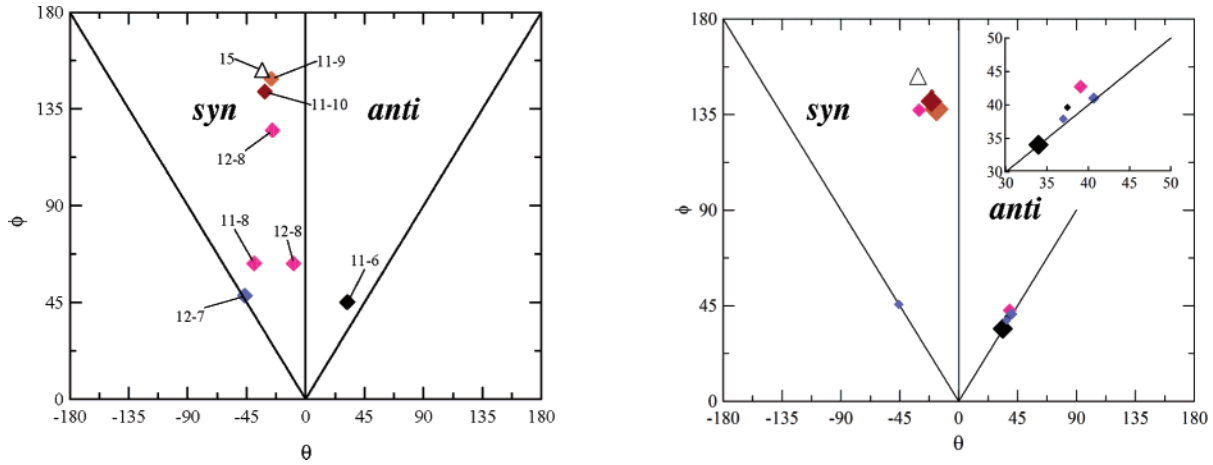

Figure 3. Ramachandran type plots describing the conformations of bisindolylmaleimides in which perfectly C_2- and C_s-symmetrical regions of conformational space are indicated by the diagonal lines. Note that only one of each degenerate conformation is shown in each case. Macrocycles **11-*n*** and **12-*n***, solid diamond; untethered compounds (**15**, left panel; **17**, right panel), triangle. The length of the tether is indicated by the color: $n = 6$, black; $n = 7$, blue; $n = 8$, magenta; $n = 9$, orange; and $n = 10$, brown. Left: Summary of conformers observed in X-ray crystal structures. The crystal structure of **12-8** was disordered, and both conformations are indicated. Right: Low-lying conformers of the macrocycles **12-*n*** identified by molecular modeling; the areas of the diamonds correspond roughly to the relative populations of each conformer. The inset shows an expanded region of the Ramachandran type plot.

38° and 43°, reflecting the compromise between conjugation and unfavorable steric interactions[35] between the indole rings; see Tables S3 and S4. Compression of the inter-aryl dihedral angles may, however, be necessary to accommodate a shorter tether. For **12-6**, for example, two low-lying anti conformers were identified by molecular modeling, the more stable of which was C_2-symmetrical and highly conjugated (θ and $\phi = 34°$). The highly conjugated nature of this conformer may account for the shifting of λ_{max} in absorption and emission spectra compared to compounds with longer tethers; see Figure 1 and Table S1.

The relative populations of the syn and anti conformers of the bisindolylmaleimides were determined using a combination of methods (see Table 3). The conformers are in fast exchange on the NMR time scale at room temperature,[36] and the observed chemical shifts are, therefore, weighted averages of those of the populated conformers. In addition, the relative free energies of conformers was predicted using molecular modeling using MP2/6-31G*//B3LYP/6-31G* (see Tables S4 and S5).

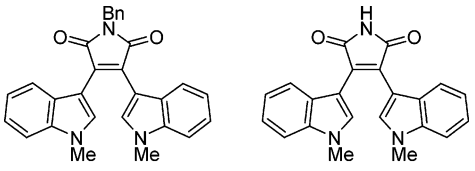

16 **17**

Table 3. Relative Populations of syn and anti Conformations of the Bisindolylmaleimides

		NMR spectroscopy		molecular modeling[a]
entry	compound	solvent	ratio syn:anti	ratio syn:anti
1a	**11-6**	CD_2Cl_2	<5:>95[b]	
1b	**12-6**	$CDCl_3$	<5:>95[b]	<0.01:>99.99
2a	**11-7**	CD_2Cl_2	30:70[b]	
2b	**12-7**	$CDCl_3$	30:70[b]	28:72
3a	**11-8**	CD_2Cl_2	50:50[b]	
3b	**12-8**	$CDCl_3$	60:40[b]	51:49
4a	**11-9**	CD_2Cl_2	>95:<5[b]	
4b	**12-9**	$CDCl_3$	>95:<5[b]	>99.99:<0.01
5a	**11-10**	CD_2Cl_2	>95:<5[b]	
5b	**12-10**	$CDCl_3$	85:15[b]	>99.99:<0.01[c]
6	**17**			98:2

[a] Populations derived from MP2/6-31G*//B3LYP/6-31G* free energies and degeneracies; the calculations were performed on the bisindolylmaleimides **12-*n*** and **17**, but the remote imide substituent in the corresponding bisindolylmaleimides **11** and **16** is unlikely to impact significantly on the ratio of conformers in solution. [b] Estimated from the chemical shifts of the indole protons. [c] The computationally expensive frequency calculations were not performed; it is clear that there is a significant (~4−5 kcal mol^{-1}) preference for the syn conformer.

The length, *n*, of the tether has an important effect on the ratio of syn and anti conformers of the bisindolylmaleimides **11** and **12**; see Table 3. The principal effect of a short tether is to destabilize the syn conformer relative to the anti and to compress the inter-ring torsion angles of the anti conformer (Figure 4). The syn conformer is preferred for both unstrained macrocycles and untethered bisindolylmaleimides and is destabilized in macrocycles with shorter tethers. With $n = 8$, the shortened tether ($n < 8$) is unable to bridge between the indole nitrogens of the syn conformation without distortion from the tether-free (idealized) geometry; with $n = 6$ and 7, unfavorable steric interactions in the syn conformer are sufficient to force the alternative anti conformer to become the ground state.

3. Rationalization of the Inhibition of Protein Kinases by Macrocyclic Binsindolylmaleimides

With some insight into the conformational preferences of the bisindolylmaleimides, we sought to rationalize their relative

(31) Davies, S. P.; Reddy, H.; Caivano, M.; Cohen, P. *Biochem. J.* **2000**, *351*, 95.
(32) Foresman, J. B.; Frisch, A. *Exploring Chemistry with Electronic Structure Methods*, 2nd ed.; Gaussian Inc., Pittsburgh, PA, 1993.
(33) (a) Hobza, P.; Sponer, J.; Reschel, T. *J. Comput. Chem.* **1995**, *16*, 1315. (b) Ujaque, H.; Lee, P. S.; Houk, K. N. Hentemann, M. F.; Danishefsky, S. J. *Chem.—Eur. J.* **2002**, *8*, 3423.
(34) For recent examples, see: (a) Hobza, P.; Riehn, C.; Weichert, A.; Brutschy, B. *Chem. Phys.* **2002**, *283*, 331. (b) Wang, Y. L.; Hu, X. C. *J. Am. Chem. Soc.* **2002**, *124*, 8445. (c) Kovács, A.; Szabó, A.; Nemcsok, D.; Hargittai, I. *J. Phys. Chem. A* **2002**, *106*, 5671. Raymo, F. M.; Bartberger, M. D.; Houk, K. N.; Stoddart, J. F. *J. Am. Chem. Soc.* **2001**, *123*, 9264.
(35) For a discussion of the conformation of biphenyl derivatives, see: Mislow, K.; Glass, M. A. W.; O'Brien, R. E.; Rutkin, P.; Steinberg, D. H.; Weiss, J.; Djerassi, C. *J. Am. Chem. Soc.* **1962**, *84*, 1455.
(36) Bartlett, S.; Nelson, A. *Chem. Commun.* **2004**, 1112. Barrett, S.; Bartlett, S.; Bolt, A.; Ironmonger, A.; Joce, C.; Nelson A.; Woodhall, T. *Chem.—Eur. J.* **2005**, *11*, in press.

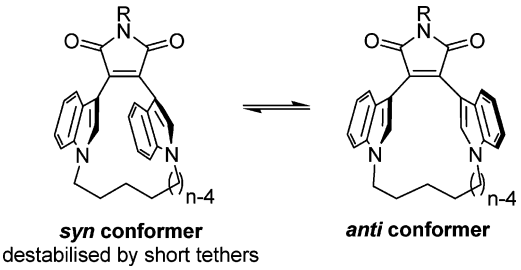

Figure 4. Summary of factors which destabilize the syn conformation of the macrocycles **11** and **12**.

inhibition of a range of protein kinases. There are no crystal structures of any of the isoforms of PKC, despite its early discovery and its importance in cancer research. The inhibition profile of a protein kinase, for example PKCβ, against the bisindolylmaleimides **12-*n*** ($n = 6-10$) can, however, reveal details of the geometry of its ATP binding site in the absence of structural information. For the inhibition of PKCβ, the tether in the most potent inhibitor, **12-6**, serves two purposes: (a) it destabilizes the otherwise low-lying syn conformer relative to the anti, and (b) it reduces the inter-ring torsion angles of the anti conformer. Both of these factors may have an important effect on the potency of the compound. The bisindolylmaleimide **12-6** is considerably more active than the analogues **12-9** and **12-10** (which populate the syn conformer predominantly), suggesting that its anti conformation is best preorganized to bind to PKCβ. Nevertheless, given that **12-9** populates essentially only the syn conformer and that its anti conformer is effectively inaccessible at room temperature, it is a surprisingly good PKCβ inhibitor (with $K_i = 160$ nM): we suggest, therefore, that some bisindolylmaleimides (such as **12-9**) may bind to PKCβ, albeit less tightly, in an undistorted syn conformation. These deductions reveal some critical information about the ATP binding site of PKCβ which may be fed into the design of, and may be used to rationalize the activity of, potent inhibitors.

The free energy profiles for the complexation of the bisindolylmaleimides **12-6** and **12-9** to PKCβ are illustrated schematically in Figure 5. The bisindolylmaleimide **12-9** almost exclusively populates the syn conformation: isomerization to the less stable anti conformer incurs a severe energetic penalty, and a complex involving a syn-oriented bisindolylmaleimide may, as a consequence, be formed; see panel B, Figure 5. In contrast, the cost of isomerization to a preorganized anti conformer has already been paid in the preparation of **12-6**, for which the anti conformer is the ground state, and higher affinity for the kinase is observed, panel A.

The bisindolylmaleimides **12-7** and **12-8** also populate the anti conformer significantly but are markedly (20- and 6-fold, respectively) less potent PKCβ inhibitors than **12-6**. The wider inter-ring torsion angles of the anti conformers of **12-7** and **12-8** (θ and $\phi = 38°-43°$) deviate significantly from the preorganized, compressed conformation of **12-6**. In addition, the syn conformer of **12-7**, in particular, is very distorted, preventing efficient formation of a complex in which the ligand adopts the alternative syn conformation (as we have proposed for **12-9**, above). Compression of the inter-ring torsion angles of the anti conformer would result in increased steric interaction between the indole rings, a price which has already been paid in the preparation of **12-6**.

The inhibition profiles of some other AGC group protein kinases (MSK1, p70 S6K, PDK1, MAPKAP-K1α, and PKCα) are similar to that observed for PKCβ, although the inhibition constants are considerably lower in absolute terms; see Figure 6 and Table S2, Supporting Information. With each of these enzymes, the bisindolylmaleimides **12-6** and **14**, which both have six-atom tethers, are the most potent inhibitors, though significant levels of inhibition are observed with the higher homologues **12-*n***, $n = 7-10$. This analysis indicates that these protein kinases also bind most tightly to the bisindolylmaleimide ligands which are preorganized in a compressed, approximately C_2-symmetric conformation.

Protein kinase A,[26] PKA, and its mutants[40] have been used as model systems for studying PKC inhibitors. This approach has been adopted largely because crystallization conditions for PKA are well established and because of the close relationship between the enzymes. A triple mutant of PKAα has been proposed as a useful surrogate for PKC, and its structure in complex with the bisindolylmaleimide **10** has been determined.[26]

Analysis of the inhibition profile of the bisindolylmaleimides **12-*n*** provides an alternative method for comparing the ATP binding sites of protein kinases. Despite their rather distant relationship in evolutionary terms, the reasonably similar inhibition profiles of PDK-1 and PKCα suggest that PDK-1 may be a useful surrogate for studying PKC inhibitors;[27] indeed, PKCβ-like mutants of PDK-1 have been studied by X-ray crystallography in an attempt to understand the molecular mechanism of PKCβ inhibition by the bisindolylmaleimides **6** and **8**−**10**.[27]

In contrast, PKA is only weakly inhibited by the bisindolylmaleimides **12-*n***, and it is difficult to draw firm conclusions about the optimal preorganization of bisindolylmaleimide PKA inhibitors. This observation may also suggest that this enzyme may be a less valuable surrogate for investigating the mechanism of action of PKC inhibitors despite the much closer relationship between the enzymes in evolutionary terms. Inhibition profiling can, therefore, be used to provide a useful comparison between protein kinases which, unlike sequence alignment, focuses on similarities between the ATP binding sites.

An interesting observation concerned the inhibition of glycogen synthase kinase-3β (GSK3β). The bisindolylmaleimides **12-8** and **12-9** were about 10-fold selective for GSK3β over all of the other kinases screened, Table 2. Given that **12-10** is less potent than **12-8** and **12-9**, it seems likely that the ability to populate a distorted syn conformation may increase affinity for the enzyme. With **12-8** and **12-9**, a rather shallow potential landscape may be accessible which may allow com-

(37) Magde, J.; Brannon, J. H.; Cremers, T. L.; Olmsted, J. *J. Phys. Chem.* **1979**, *83*, 696.
(38) Ben-Amotz, D.; Harris, C. B. *J. Chem. Phys.* **1987**, *86*, 4856.
(39) Hanks, S. K.; Hunter, T. In *The Protein Kinase FactsBook, Part I: Protein-Serine Kinases*; Hardie, G., Hanks, S., Eds.; Academic Press: London, 1995; p 7.
(40) (a) Toullec, D.; Pianetti, P.; Coste, H.; Bellevergue, P.; Grand-Perret, T.; Ajakane, M.; Baudet, V.; Boissin, P.; Boursier, E.; Loriolle, F. *J. Biol. Chem.* **1991**, *266*, 15771. (b) Davis, P. D.; Hill, C. H.; Keech, E.; Lawton, G.; Nixon, J. S.; Sedgwick, A. D.; Wadsworth, J.; Westmacott, D.; Wilkinson, S. E. *FEBS Lett.* **1989**, *259*, 61. (c) Davis, P. D.; Elliott, L. H.; Harris, W.; Hill, C. H.; Hurst, S. A.; Keech, E.; Kumar, M. K.; Lawton, G.; Nixon, J. S.; Wilkinson, S. E. *J. Med. Chem.* **1992**, *35*, 994. (d) Davis, P. D.; Hill, C. H.; Lawton, G.; Nixon, J. S.; Wilkinson, S. E.; Hurst, S. A.; Keech, E.; Turner, S. E. *J. Med. Chem.* **1992**, *35*, 177. (e) Bit, R. A.; Davis, P. D.; Elliott, L. H.; Harris, W.; Hill, C. H.; Keech, E.; Kumar, H.; Lawton, G.; Maw, A.; Mixon, J. S.; Vesey, D. R.; Wadsworth, J.; Wilkinson, S. E. *J. Med. Chem.* **1993**, *36*, 21.

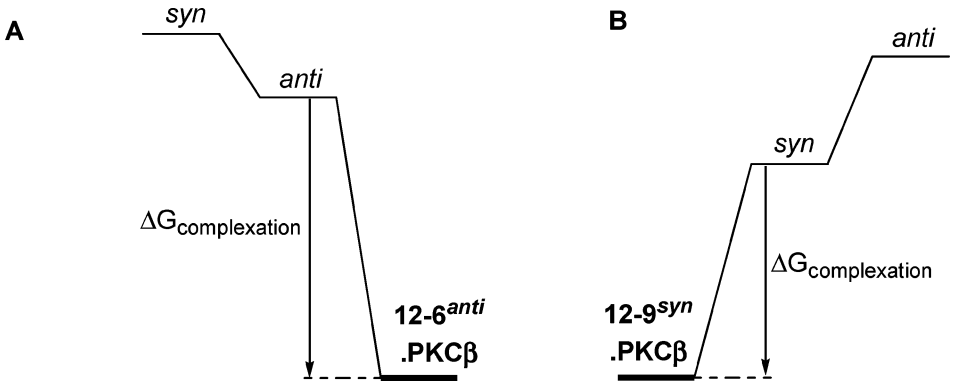

Figure 5. Schematic free energy profile illustrating the complexation of bisindolylmaleimides with PKCβ. The relative free energies of the syn and anti conformers in solution (black) are shown relative to the protein−ligand complexes (bold). (Panel A) Complexation of bisindolylmaleimide **12-6**, which is preorganized in an anti conformation, to PKCβ. (Panel B) Complexation of the bisindolylmaleimide **12-9** to PKCβ.

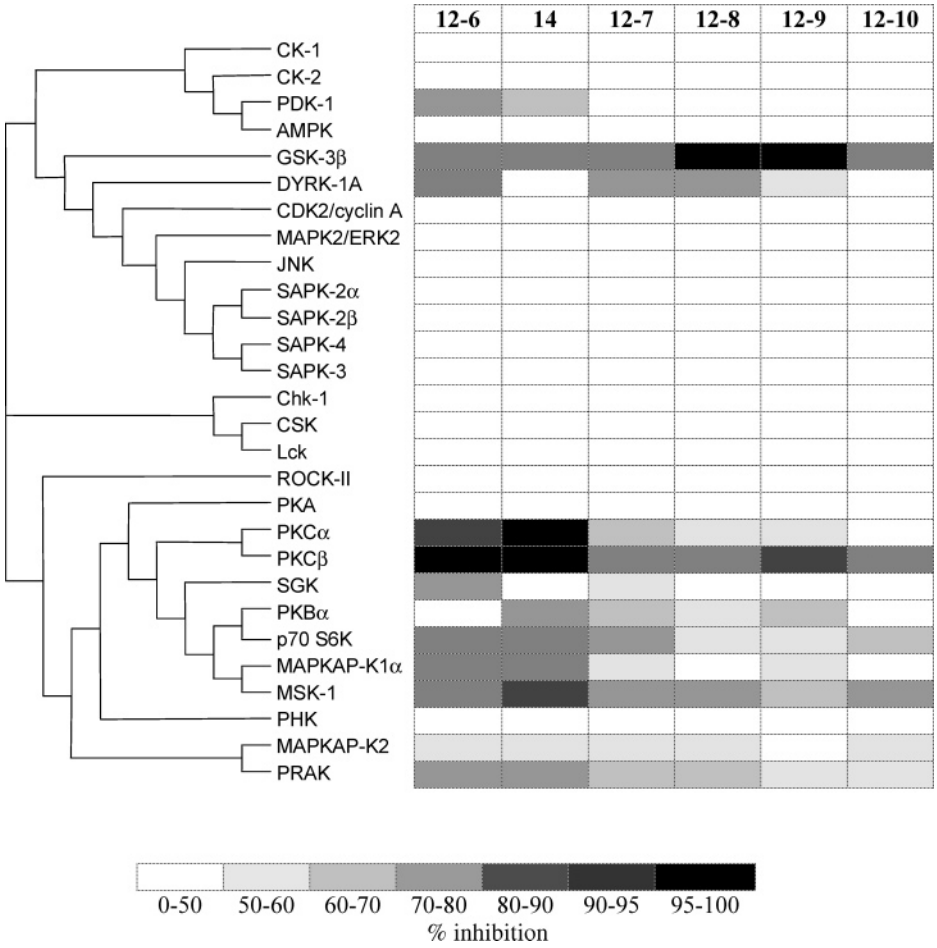

Figure 6. Phylogenetic relationship[39] between, and inhibition profile of, protein kinases. (Left) Phylogenetic tree. (Right) Inhibition profiles (% inhibition with 10 μM inhibitor) with the bisindolylmaleimide inhibitors: **12-*n*** and **14**. The abbreviations are sumamarized in the Supporting Information.

plexation to GSK3β. The bisindolylmaleimides **7** are known inhibitors of GSK3β ($n = 1$, $IC_{50} = 0.136$ μM; $n = 2$, $IC_{50} = 0.022$ μM; $n = 3$, $IC_{50} = 0.026$ μM). Interestingly, the most potent of the inhibitors **7** ($n = 2$ and 3), which have eleven- and fourteen-atom tethers, respectively, may also populate a distorted syn conformation since the chemical shifts of the indole protons of the inhibitors **7** ($n = 2$ and 3) correlate well with those of **12-8** and **12-9** (Figure S4, Supporting Information). The proposed bound (syn) conformation of potent inhibitors of GSK3β conflicts with a model previously presented.[20]

4. Analysis of the Conformation of Bisindolylmaleimides in Complex with Protein Kinases

The structures of the complexes of PKA[26] with **10** and PDK-1[27] with **6**, **8**, **9a**, **9b**, and **10** have recently been determined and offer an opportunity to validate the use of inhibition profiling to infer the optimal preorganized conformation of a ligand. Our previous analysis concluded that higher affinity bisindolylmaleimides would be preorganized to bind PDK-1 in a compressed, anti conformation, and that undistorted macrocyclic ligands would bind to the enzyme in an unsymmetrical syn conforma-

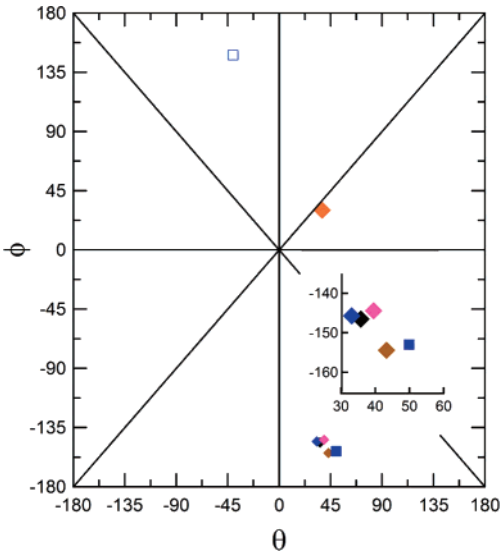

Figure 7. Ramachandran type plots describing the conformations of bisindolylmaleimides in complex with protein kinases. The diagonal lines correspond to perfectly C_2- and C_s-symmetrical regions of conformational space; regions of the plot related by reflection in these lines map ligand conformations related by rotational and reflectional symmetry, respectively. Bisindolylmaleimides complexed to PDK-1, diamond, and to PKA, square. The complex of the bisindolylmaleimide **10** cocrystallized with PKA as an asymmetric pair of kinase-inhibitor complexes, both of which are shown; PKA was in an inactive conformation in one of these complexes, open square. The ligands are indicated by color: **6**, orange; **8**, black; **9a**, magenta; **9b**, brown; and **10**, blue. The PDK-1-bound conformation of **6** is related to those of **8**, **9a**, **9b**, and **10** by rotation through approximately 180° about one of its maleimide−indole bonds (defined by ϕ).

tion. This conclusion is largely supported by structural evidence. The optimized ligand **6**, in which the indole nitrogens are linked by a six-atom tether, binds PDK-1 in an anti conformation, Figure 7: the conformation is unsymmetrical (with $\theta = 38°$ and $\phi = 31°$), with one of the indoles highly conjugated with the maleimide ring. The bisindolylmaleimides **8**, **9a**, **9b**, and **10**, on the other hand, are not constrained in a macrocyclic ring, and their ground state is likely to be an undistorted syn conformation which is similar to that of the parent compound **15**: these compounds bind to PDK-1 in syn conformations which are close to their ground state ($\theta = 33°$ to 43° and $\phi = -155°$ to $-145°$). The alternative conformations of bound bisindolylmaleimides occupy similar regions of three-dimensional space and are simply related by rotation through approximately 180° about the maleimide−indole bond of the more conjugated indole ring of **6**. This operation leaves the (rotated) indole ring in the same plane (and similarly conjugated with the maleimide) in a conformation which resembles the ground state of unlinked compounds (including **8**−**10**). Although the bisindolylmaleimides **8**−**10** are less potent inhibitors of PDK-1 than **12-6**, they are still preorganized to bind to the kinase, but in the alternative syn bisindolylmaleimide conformation.

The bisindolylmaleimide **10** was shown to cocrystallize with PKA as an asymmetric pair of kinase-inhibitor complexes.[26] The ligand binds tightly to one of the kinase molecules via an induced fit in its ATP binding pocket; although the kinase is partially open with respect to the catalytic conformation, the inhibitor adopts the undistorted syn bisindoylmaleimide conformation which is very similar to that observed for the complexes of PDK-1.[27] The conformation of the other kinase, which may be catalytically inactive,[27] is much more open, and the bisindolylmaleimide ring system of the inhibitor adopts the enantiomeric, undistorted syn conformation (the conformation of the inhibitor as a whole is diastereomeric because of the remote stereogenic center on its substituent). This alternative inhibitor conformation does not, presumably, provide insight into the mechanism of competitive inhibition of protein kinases.

Table 4. Interaction Energies between Low-Lying Conformers of the Bisindolylmaleimides **12-*n*** ($n = 6-9$) for the Lowest Energy Conformation that Adopts the Experimental Maleimide Binding Mode and the PDK-1•**6** Protein Structure [and the PDK-1•**10** Protein Structure in Parentheses][a]

	interaction energy/kcal mol^{-1}			
conformer	**12-6**	**12-7**	**12-8**	**12-9**
anti(1)	−37.9 (5) [−36.0 (5)]	−35.5 (3) [−36.8 (5)]	−37.5 (2) [−37.6 (5)]	*c*
ent-anti(1)	−35.4 (5) [−31.0 (5)]	−27.2[b] (4) [−30.2 (5)]	−12.3[b] (0) [−30.0 (5)]	*c*
anti(2)	*c*	−30.7 (4) [−36.1 (5)]	*c*	*c*
ent-anti(2)	*c*	−26.5 (5) [−29.0 (2)]	*c*	*c*
syn(1)	*c*	−28.3[b] (0) [−25.0[b] (2)]	−15.3[b] (0)[c] [−18.3[b] (0)][c]	−5.0[b] (0) [NA[d]]
ent-syn(1)	*c*	−20.2[b] (0) [−28.2[b] (2)]	−24.6 (1)[c] [−27.0 (4)][c]	NA[d] [−33.0 (5)]
syn(2)	*c*	*c*	−6.5[b] (0) [−30.5 (1)]	−2.0[b] (0)[c] [−25.8[b] (2)][c]
ent-syn(2)	*c*	*c*	NA[d] [NA[d]]	−30.0 (1)[c] [−37.3 (5)][c]

[a] The number of the top five solutions in which the maleimide binding mode was replicated is indicated in parentheses. [b] Highest ranked solution for this conformer did not replicate the maleimide binding mode. [c] Conformer not significantly (>2%) populated at room temperature. [d] no solution found in the maleimide binding mode.

To gain insight into the inhibition of the AGC family of protein kinases, docking studies involving the bisindolylmaleimides **12-*n*** ($n = 6-9$) were undertaken using protein structures of PDK-1 in complex with the bisindolylmaleimides **6** and **10**. In the current study, both enantiomers of all accessible, low-lying conformations identified using B3LYP/6-31G* were docked to the protein (which was treated as rigid). The program Q-fit[41] was used for docking, though the macrocyclic nature of the ligands permitted only rigid body docking. In each case, the objective was to determine which low-lying conformations docked to a given protein. The resulting protein−ligand complexes were manually inspected for hydrogen bonding contacts with Ser160, Ala162, and Thr222 which are enjoyed by other bisindolylmaleimides. Pleasingly, the highest ranking solutions for docking into the PDK-1•**6** protein structure were those bisindolylmaleimides which had been docked in an anti conformation which had the same absolute configuration as the bisindolylmaleimide ligand in the crystal structure (see Table 4). Where no low-lying anti conformer was available, as in **12-9**, a syn conformer could be docked productively, although much less favorably, onto the PDK-1•**6** protein structure (see *ent-syn*(1) and *ent-syn*(2), Table 4). The interaction of syn conformers of **12-9** was rendered significantly more favorable by docking onto the alternative PDK-1 conformation observed in the PDK-1•**10** protein structure. Figure 8 shows the bisindolylmaleimides **12-6** and **12-9** in complex with PDK-1 in anti and syn conformations, respectively. The results demonstrate the

(41) Jackson, R. M. *J. Comput. Mol. Des.* **2002**, *16*, 43.

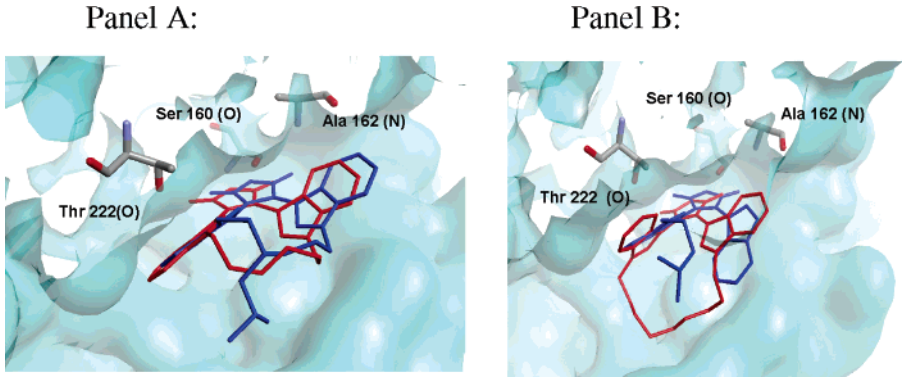

Figure 8. Bisindolylmaleimides docked onto the protein structures. The ligands are indicated by color: **6** (red) and **12-*n*** (blue). (Panel A) **12-6** docked in a low-lying anti conformation onto the PDK-1•**6** complex; the absolute configuration of the docked conformer is the same as that observed in the PDK-1•**6** crystal structure. (Panel B) **12-9** docked in a low-lying syn conformation onto the PDK-1•**10** complex; the absolute configuration of the docked conformer is the same as that observed in the PDK-1•**10** crystal structure.

importance of conformational change in the protein binding site as well as ligand conformation. There would appear to be a protein induced-fit mechanism in PDK-1 which allows binding of both the anti and syn conformers of the bisindolylmaleimides **12**.

The docking of the bisindolylmaleimides **12-*n*** ($n = 6-9$) onto GSK-3β is greatly complicated by the induced fit mechanism which the protein exploits to optimize ligand binding (see Figure S2, Supporting Information, for an overlay of the twelve currently available crystal structures of GSK-3β). However, docking studies involving GSK-3β protein structures[9,42] may provide some insight into why **12-8** and **12-9** are the most potent inhibitors of this enzyme. The results for ligand docking onto two different unbound protein structures of GSK3β (1H8F and 1I09) differ from being completely unable to recreate the maleimide binding mode (in 1H8F) to the recreation of the hydrogen bonding contacts observed in GSK3β•ligand complexes (in 1I09). With the second unbound structure, 1I09, the top energy ranked solutions involved two syn conformers of **12-9** (see *ent-syn*(1) and *ent-syn*(2), Table 5); although these solutions did not completely recreate all of the usual hydrogen-bonding contacts with the maleimide, it is likely that the flexible loop which forms part of the ATP binding pocket may adjust to optimize favorable interactions with different ligands. The unbound structure can be considered a ground-state for the protein. Therefore, the observed preference for the **12-8** and **12-9** syn conformers contrasts with PDK-1 where the preference is for anti conformers. This important conclusion was also reached by analyzing the inhibition profiles (see Figure 6) with reference to the conformation analysis of the bisindolylmaleimides described above.

Given the high level of conformational flexibility in the nucleotide-binding loop (residues 61−71) in different GSK-3β structures (Figure S2), docking was undertaken to the unbound structure (1I09) with this loop region removed. The results show that, even without the loop, GSK-3β retains a slight preference for syn conformers of **12-8** and **12-9** (see *ent-syn*(1) and *ent-syn*(2), Table S4, Supporting Information).

Table 5. Interaction Energies between Low-Lying Conformers of the Bisindolylmaleimides **12-*n*** ($n = 6-9$) and a GSK-3β Protein Structure (1I09)[a]

	interaction energy/kcal mol^{-1}			
conformer	**12-6**	**12-7**	**12-8**	**12-9**
anti(1)	−28.2[b] (3[c])	−28.0[c] (2[c])	−26.3[b,c] (1)	*d*
ent-anti(1)	−29.4 (2)	−30.5 (2)	−29.6 (1)	*d*
anti(2)	−29.0[c] (5[c])	−28.7[c] (4[c])	*d*	*d*
ent-anti(2)	−29.7 (2)	−29.7 (2)	*d*	*d*
syn(1)	*d*	−26.0[b] (2[c])	NA[b] (0)[d]	−20.4[b] (0)
ent-syn(1)	*d*	−27.9[c] (3[c])	−28.8[c] (5[c])[a]	−31.1[c] (5[c])
syn(2)	*d*	*d*	−25.5[b] (0)	−29.3[b,c] (2)[d]
ent-syn(2)	*d*	*d*	−22.9[b] (0)	−32.0[c] (5[c])[d]

[a] The number of the top five solutions in which the maleimide binding mode was replicated is indicated in parentheses. [b] Highest ranked solution for this conformer did not replicate the maleimide binding mode. [c] The solution did not recreate all of the hydrogen bonds in the usual maleimide binding mode. [d] Conformer not significantly (>2%) populated at room temperature.

5. Summary

The series of macrocyclic bisindolylmaleimides (**12-*n*** and **14**) described in this study have been shown to populate quite distinct regions of conformational space. Inhibition profiling using this series of compounds may be used to probe the ATP binding sites of a particular protein kinase and to compare the active sites of different protein kinases. This approach was used to compare the ATP binding sites of a range of protein kinases and to demonstrate that PDK-1 (and its mutants) may be good surrogates for the study of PKC inhibitors. Furthermore, the approach focuses on the comparison of the active sites of protein kinases in a manner and, like sequence alignment, also does not require structural information. Although PKCα and PDK-1 are rather distant relations in evolutionary terms, the ATP binding site of PDK-1 (and its mutants) may be a better surrogate for PKCα than is the more closely related protein kinase, PKA.

By screening against a panel of conformationally diverse bisindolylmaleimides, it was also possible to infer how the conformation of a bisindolylmaleimide should be preorganized to inhibit different protein kinases. This approach leads to the conclusion that several AGC group protein kinases (including PKCα, PKCβ, MSK1, p70 S6K, PDK-1, and MAPKAP-K1α) may be best inhibited by bisindolylmaleimides which adopt a

(42) (a) Dajani, R.; Fraser, E.; Roe, S. M.; Young, N.; Good, V.; Dale, T. C.; Pearl, L. H. *Cell* **2001**, *105*, 721. (b) Meijer, L. et al. *Chem. Biol.* **2003**, *10*, 1255. (c) Bax, B.; Carter, P. S.; Lewis, C.; Guy, A. R.; Bridges, A.; Pettman, R.; Tanner, G.; Mannix, C.; Culbert, A. A.; Brown, M. J. B.; Smith, D. G.; Reith, A. D. *Structure* **2001**, *9*, 1143. (d) Ter Haar, E.; Coll, J. T.; Austen, D. A.; Hsiao, H.-M.; Swenson, L.; Jain, J. *Nat. Struct. Biol.* **2001**, *8*, 593. (e) Aoki, M.; Yokota, T.; Sugiura, I.; Sasaki, C.; Hasegawa, T.; Okumura, C.; Kohno, T.; Sugio, S.; Matsuzaki, T. *Acta Crystallogr. D* **2004**, *60*, 439. (f) Dajani, R.; Fraser, E.; Roe, S. M.; Yeo, M.; Good, V.; Thompson, V.; Dale, T. C.; Pearl, L. H. *EMBO J.* **2003**, *22*, 494.

compressed, approximately C_2-symmetric anti conformation; in constrast, GSK3β is best inhibited by bisindolylmaleimides whose ground state is a distorted syn conformation. Compounds such as **12-*n*** and **14** may, therefore, serve as valuable starting points in the design of more potent and selective kinase inhibitors of therapeutic and biological importance.

The bisindolylmaleimides **12-*n*** and **14** are achiral and generally populate two enantiomeric conformations (rather than a single *meso* conformation); their biological activity might be optimized, as LY333531, **6**, has been honed for PKCβ inhibition, by the introduction of substituents to the tether. This process would render the alternative conformations diastereoisomeric and could improve selectivity by restricting the regions of conformational space which may be populated by the unbound inhibitor.

6. Experimental Section

Proton NMR spectra were recorded on a Bruker DRX 500 Fourier transform spectrometer using an internal deuterium lock; chemical shifts are quoted in parts per million downfield of tetramethylsilane. Enzyme inhibition data was fitted to the equations for competitive and noncompetition inhibition using the suite of programs described by Cleland.[30] The specificity of the bisindolylmaleimides **11-*n***, **12-*n***, **14**, and **15** was profiled against a panel of protein kinases as has been previously described.[31]

The fluorescence quantum yields were determined as previously described.[43] The populations and lifetimes of the excited singlet state were determined by time-correlated, single-photon counting using a cavity-dumped, mode-locked, dye-laser as the excitation source and a Hamamatsu Microchannel Plate photomultiplier with Becker & Hickel electronics to detect the photons. The instrument response time is ~50 ps; decays were measured with 54.7° polarization to remove rotational diffusion. The decays were analyzed using a sum of exponential terms $I(t) = \sum_i^3 a_i \exp(-t/\tau_i) + c$ using as few terms as possible in each case. Where necessary, convolution with a measured instrument function was also performed.

All of the quantum mechanical calculations were performed with the Gaussian 98 suite of programs. All minima were verified by frequency calculations at the B3LYP/6-31G* level (apart from **12**−**10**) which showed no negative frequencies. MP2/6-31G* single-point energy evaluations were performed using B3LYP/6-31G*-optimized geometries. Enthalpy and entropy calculations used unscaled frequencies.

Low-lying conformations of the bisindolylmalimides **12-*n*** (n = 6−10) were identified from a conformational search (MMFF force field) using PC Spartan Pro 1.0. The two lowest lying conformations for each of the syn and anti conformers according to the force field were reoptimized using B3LYP/6-31G* which has been shown to reproduce molecular geometries and energies well.[32] This method has previously been shown to be poor at reproducing weak intermolecular interactions, notably aromatic−aromatic type interactions.[33] In these molecules, such interactions may be relevant, but their intramolecular nature ensures that this will impact principally on the estimation of relative energies and not on geometries. These interactions are captured well by the MP2 methods and consequently MP2/6-31G* single-point energy evaluations have been performed on the B3LYP/6-31G* geometries.[34]

Docking studies were undertaken using Q-fit[41] which has recently been improved to provide a platform for flexible protein−ligand docking. The method uses the molecular mechanics force field GRID to score multiple ligand conformations that are oriented in an energetically favorable manner within the active site of a protein. Q-fit calculates an interaction energy between the ligand and the protein which is composed of energy terms for van der Waals, electrostatic, and hydrogen bonding. All nonprotein atoms including water molecules were removed before docking calculations were undertaken.

The kinase sequences were collected from The Protein Kinase Resource (http://pkr.sdsc.edu/html/index.shtml). The kinase sequences were used as input for the recently developed multiple alignment program MUSCLE, which is one of the most reliable and accurate programs for multiple sequence alignment available.[44] The multiple alignment of the protein kinase sequences produced a tree with high reliability when tested with bootstrap analysis using ClustalW.[45] The freely downloadable program TreeView was used to visualize the tree.[46]

Acknowledgment. We thank EPSRC, BBSRC, AstraZeneca, and the Wellcome Trust for support, the Royal Society for a fellowship (for G.D.R.), Sarah King and Alan Berry for helpful discussions, and Jenny Bain, Matthew Elliot, and David Thain (Division of Signal Transduction Therapy, School of Life Sciences, University of Dundee) for profiling the specificity of the bisindolylmaleimides **11-*n***, **12-*n***, **14**, and **15** against a panel of protein kinases.

Supporting Information Available: Complete refs 20, 23, and 42b. Tables detailing (a) the absorption/emission maxima for the bisindolylmaleimides **11-*n*** and **12-*n*** (Table S1); (b) the inhibition of a panel of 29 protein kinases by **11-*n***, **12-*n***, **14** and **15** (Table S2); (c) a summary of bisindolylmaleimide conformations identified by X-ray crystallography (Table S3); (d) a summary of low-lying conformations identified by molecular modeling (Table S4); (e) details of molecular modeling of the two lowest lying syn and anti conformers of the macrocylces **12-*n*H** using B3LYP/6-31G*//B3LYP/6-31G* and MP2/6-31G*//B3LYP/6-31G* (Table S5); (f) the interaction energies of the bisindolylmaleimides **12-*n*** (n = 6−9) and a GSK-3β protein structure (1I09) with the nucleotide-binding loop (residues 61−71) removed (Table S6); and (g) lifetimes of the excited states of macrocyclic bisindolylmaleimides **11-*n*** in chloroform (Table S7). Figures (a) of the X-ray crystal structures of bisindolylmaleimides (Figure S1); (b) illustrating the deviation of one of the carbonyl oxygens from the maleimide plane in the crystal structures of the bisindolylmaleimides **12-7** and **12-8** (Figure S2); (c) comparing the chemical shifts of the indolyl protons of the macrocycles **11-*n*** recorded in $CDCl_3$ (Figure S3); (d) comparing the chemical shifts of the indolyl protons of the GSK3β inhibitors **7** (n = 2 and 3) and **12-8** (Figure S4); and (e) showing the conformation of GSK-3β in complex with a range of inhibitors (Figure S5). A list of the B3LYP/6-31G*-optimized geometries of low-lying bisindolylmaleimide (**12-*n***) conformations is provided. This material is available free of charge via the Internet at http://pubs.acs.org.

JA050576U

(43) Parker, C. A.; Rees, W. T. *Analyst* **1960**, *85*, 587.
(44) Edgar, R. C. *Nucleic Acid Res.* **2004**, *32*, 1792.
(45) Higgins, D.; Thompson, J.; Gibson, T.; Thompson, J. D.; Higgins, D. G.; Gibson, T. J. *Nucleic Acid Res.* **1994**, *22*, 4673.
(46) Page, R. D. *Comput. Appl. Biosci.* **1996**, *12*, 357.